Electronic Supplementary Material (ESI) for Physical Chemistry Chemical Physics.

Supplementary Information

for

Vibrational Circular Dichroism towards Asymmetric Catalysis: Chiral Induction in Substrates Coordinated with Copper(II) Ions

Hisako Sato, [a*] Kazuyoshi Takimoto, [a] Jun Yoshida[b] and Akihiko Yamagishi[c]

[a] Graduate School of Science and Engineering, Ehime University, Matsuyama 790-8577, Japan, sato.hisako.my@ehime-u.ac.jp

[b] Department of Chemistry, Kitasato University, Sagamihara 252-0329, Japan

[c] School of Medicine, Toho University, Ota-ku, Tokyo 143-8540, Japan

Contents

Figures

Tables

1. UV-vis spectra of a methanol solution of [Cu(*RR*-oxa)]$^{2+}$

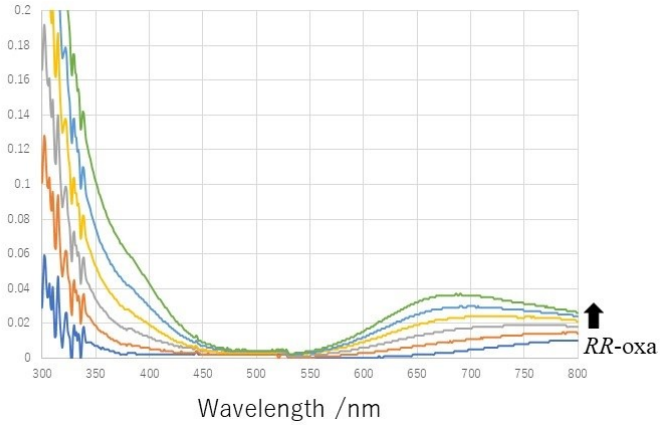

Figure S1. The change of UV-vis spectra when *RR*-oxa was added to a methanol solution of $Cu(TFMS)_2$. The initial concentration of $Cu(TFMS)_2$ was 1.2 mM. The concentration of *RR*-oxa was changed from 0 mM to 1.2 mM. The increase of the absorption band around 670 nm on adding *RR*-oxa represented the progressive formation of a chiral Cu(II) complex, [Cu(*RR*-oxa)]$^{2+}$.

2. HPLC chromatograms of $[Cu(\mathit{SS}\text{-oxa})]^{2+}$ and $[Cu(\mathit{SS}\text{-oxa})L]^{+}$

The purity of the used Cu(II) complexes was examined by means of high performance liquid chromatography (HPLC). A methanol solution of a Cu(II) complex was mounted on a C18 column and eluted by methanol containing sodium trifluoromethanesulfonate (NaTFMS).

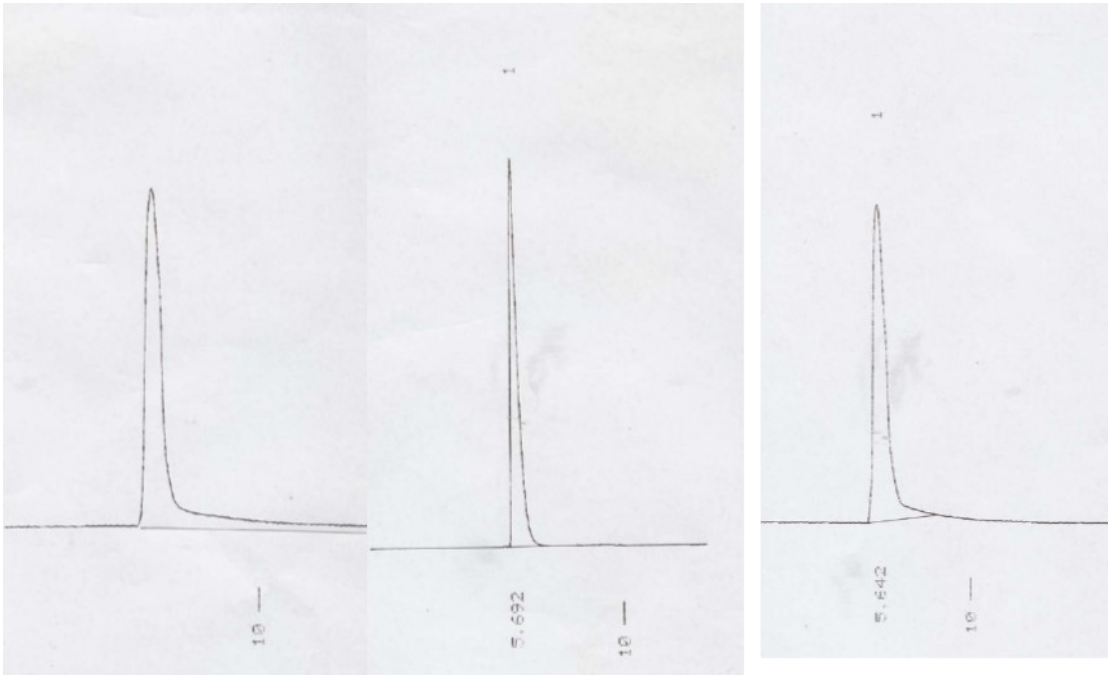

Figure S2. The HPLC chromatogram when a Cu(II) complex was eluted on a C18 column. The conditions were following: a column (CAPCELL PAK C_{18} UG, Shiseido Ind. Co. (Japan)), an eluent (methanol containing 30 mM NaTFMS), a flow rate (0.5mL min^{-1}) and wavelength (600 nm). The injected complexes were [Cu(*SS*-oxa)](TFMS)$_2$ (left), [Cu(*SS*-oxa)(bzac)](TFMS) (center) and [Cu(*SS*-L)(dbm)](TFMS), respectively. The slight tailing observed for the cases of [Cu(*SS*-oxa)](TFMS)$_2$ and [Cu(*SS*-L)(dbm)](TFMS) might be attributed to the partial decomposition of the complexes on a column.

3. Mass spectra of [Cu(*RR*- or *SS*-oxa)]$^{2+}$ and [Cu(*RR*- or *SS*-oxa)L]$^{+}$

Mass spectra were obtained for the used Cu(II) complexes. The methanol solution collected at each peak in the HPLC chromatograms (Figure S2) were measured. The results are given below comparing with the calculated ones:

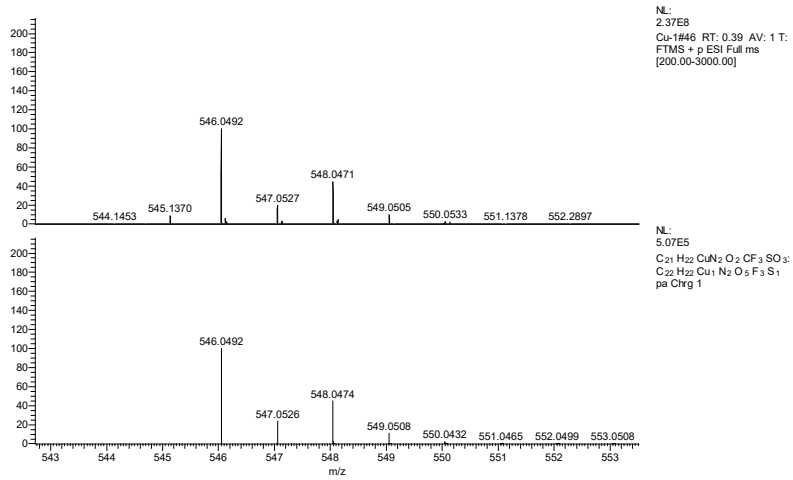

Figure S3 (a). The observed (upper) and calculated (lower) spectra of [Cu(*SS*-oxa)](TFMS)$_2$. The calculation was made for the elemental composition of $C_{21}H_{22}N_2O_2CuCF_3SO_3^+$; calc. H^+ (*m*/*z*=546.0492) and found *m*/*z*= 546.0492[M^+H^+].

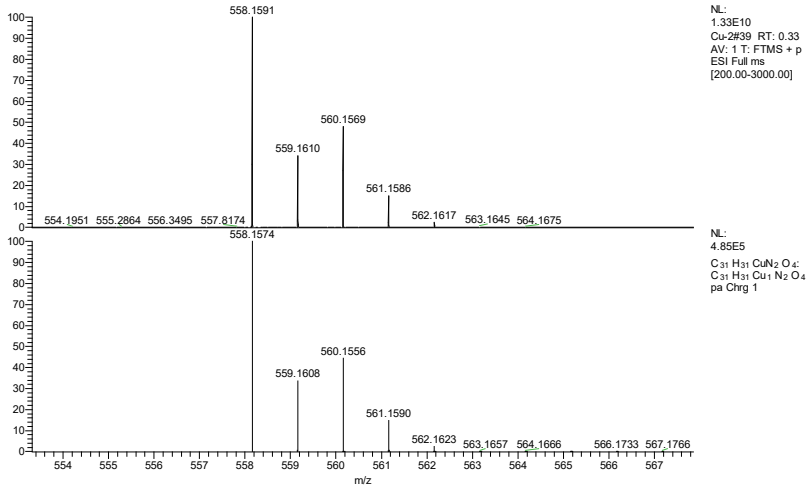

Figure S3 (b). The observed (upper) and calculated (lower) spectra of [Cu(*SS*-oxa)(bzac)](TFMS). The calculation was made for the elemental composition of $C_{31}H_{31}N_2O_4Cu^+$; calc. H^+ (*m*/*z*=558.1591) and found *m*/*z*= 558.1591[M^+H^+].

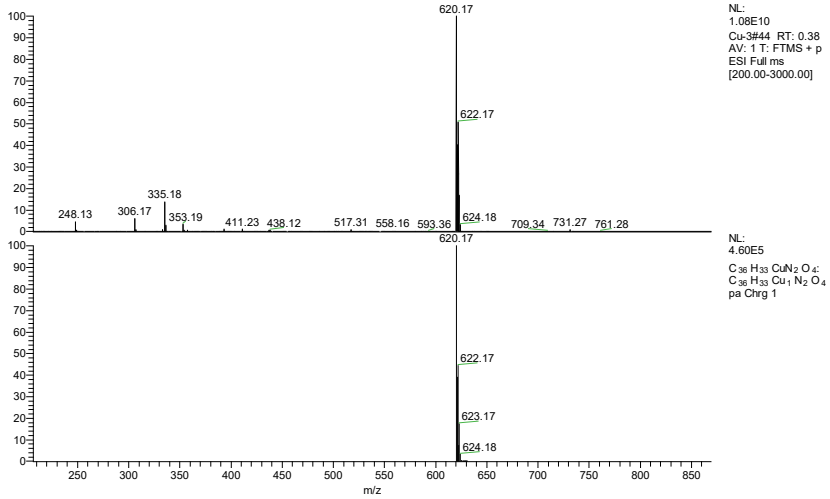

Figure S3 (c). The observed (upper) and calculated (lower) spectra of [Cu(*SS*-oxa)(dbm)](TFMS). The calculation was made for the elemental composition of $C_{36}H_{33}N_2O_4Cu^+$; calc. H^+ 620.17, found *m*/*z*= 620.17[M^+H^+].

4. Calculated VCD and IR spectra of [Cu(*SS*-oxa)]$^{2+}$, [Cu(*SS*-oxa)](TFMS)$^{+}$ and [Cu(*SS*-oxa)](TFMS)$_2$ for the optimized structures

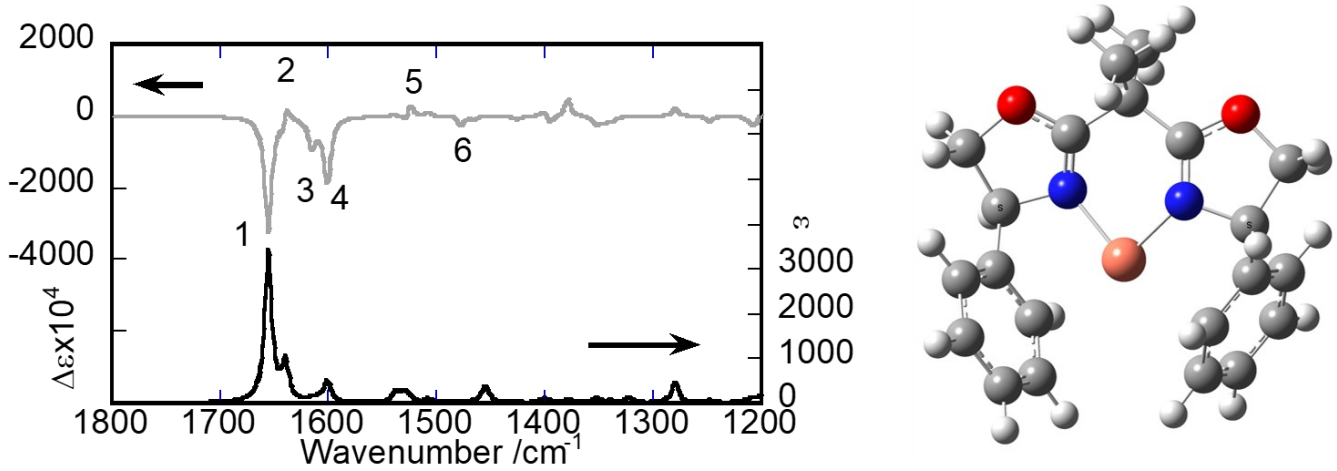

Figure S4(a). (left) The calculated IR (lower) and VCD (upper) spectra of [Cu(*SS*-oxa)]$^{2+}$ in $CHCl_3$, using the PCM model. The number of each peak corresponds to that of the observed one. (right) The optimized structure of [Cu(*SS*-oxa)]$^{2+}$ as a model of the Cu(II) complex in $CHCl_3$, using the PCM model.

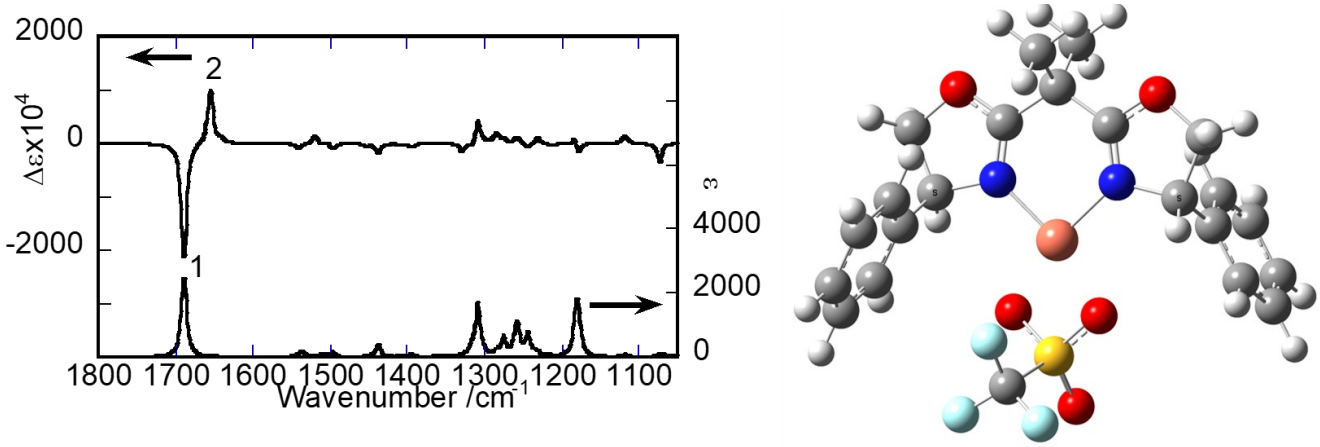

Figure S4(b). (Left) the calculated IR (lower) and VCD (upper) spectra of [Cu(*SS*-oxa)](TFMS)$^{+}$ in $CHCl_3$, using the PCM model. The number of each peak corresponds to that of the observed one. (Right) the optimized structure of [Cu(*SS*-oxa)] (TFMS)$^{+}$ as a model of the Cu(II) complex in $CHCl_3$, using the PCM model.

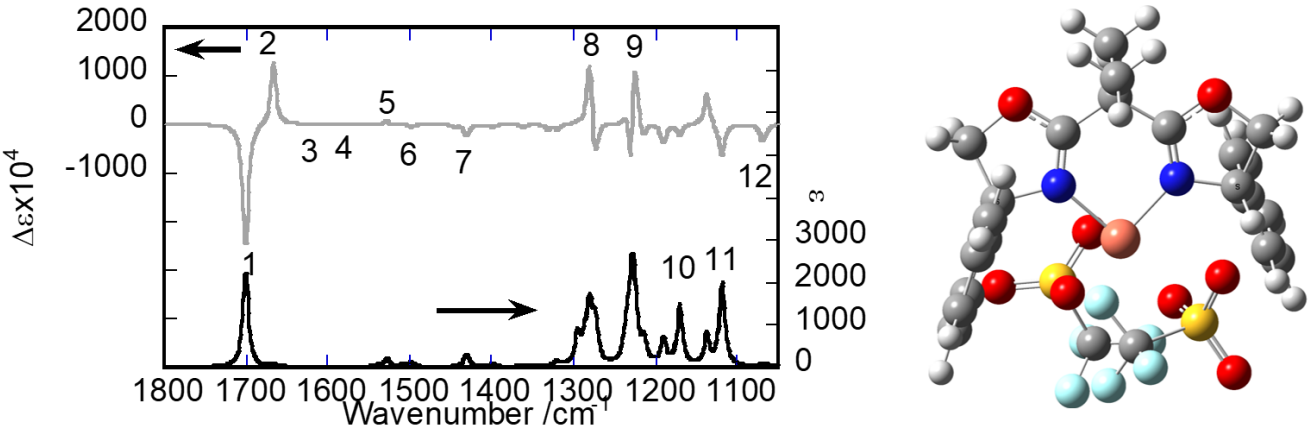

Figure S4(c). (Left) the calculated IR (lower) and VCD (upper) spectra of [Cu(*SS*-oxa)](TFMS)$_2$ in $CHCl_3$, using the PCM model. The number of each peak corresponds to that of the observed one. (Right) the optimized structure of [Cu(*SS*-oxa)](TFMS)$_2$ as a model of the Cu(II) complex in $CHCl_3$, using the PCM model.

5. Calculated VCD and IR spectra of [Cu(*SS*-oxa)(bzac)]$^{+}$ for the optimized structure

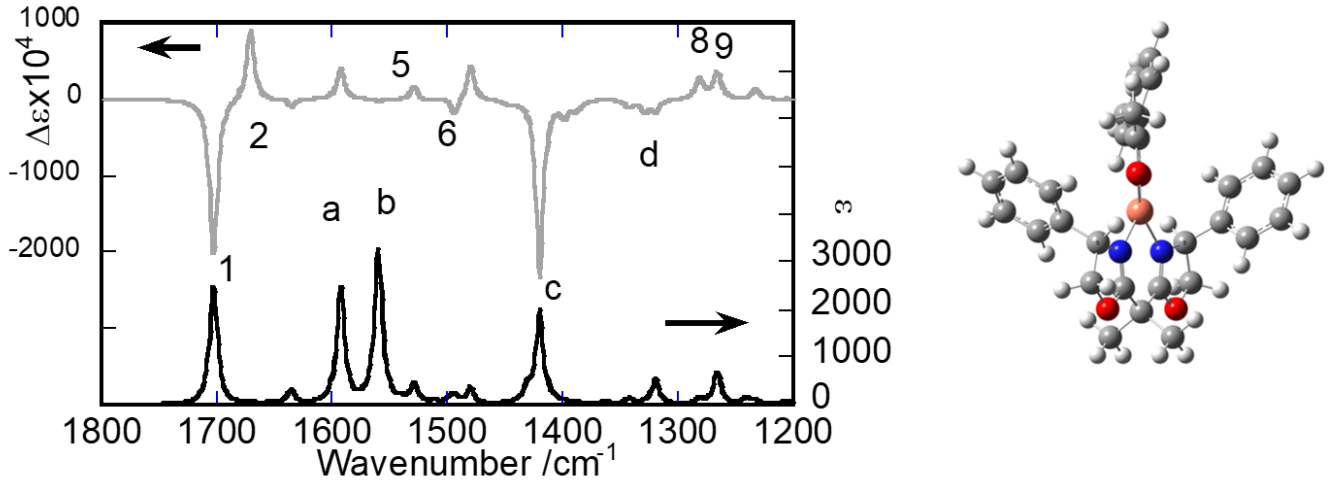

Figure S5. (Left) the calculated IR (lower) and VCD (upper) spectra of [Cu(*SS*-oxa)(bzac)]$^{+}$in $CHCl_3$, using the PCM model. The number of each peak corresponds to that of the observed one. (Right) the optimized structure of [Cu(*SS*-oxa)(bzac)]$^{+}$as a model of the Cu(II) complex in $CHCl_3$, using the PCM model.

Table S1. Assignment of the main peaks in experimental VCD spectra*

NO	[Cu(*SS*-oxa)(H_2O)$_2$] ($TFMS$)$_2$	[Cu(*SS*-oxa)(bzac)](TFMS)	[Cu(*SS*-oxa)(dbm)](TFMS)
1	ν_s C-N	ν_s C-N	ν_s C-N
2	ν_{as} C-N δ_{OH} (H_2O)	ν_{as} C-N	ν_{as} C-N
3	*vc-c-c* (phenyl group)	*vc-c-c* (phenyl group)	*vc-c-c* (phenyl group)
4	*vc-c-c* (phenyl group)	*vc-c-c* (phenyl group)	*vc-c-c* (phenyl group)
5	δ_{C-H} bending (CH_2) (scissoring)	δ_{C-H} (CH_2) (scissoring)	δ_{C-H} (CH_2) ρ_{C-H} (phenyl group) (locking)
6	ρ_{C-H} (phenyl group) ρ_{C-H} (chiral center) τ_{C-H} (CH_3)	τ_{C-H} (bzac)(CH_3) ρ_{C-H} (bzac) (phenyl group) ρ_{C-H} (phenyl group)	τ_{C-H} (CH_3) ρ_{C-H} (phenyl group)
7	ω_{CH} (wagging)	-	-
8	τ_{C-H} (twisting) ν_{as} S-O (counter anion)	τ_{C-H} ν_{as} S-O (counter anion)	τ_{C-H} ν_{as} S-O (counter anion)
9	ρ_{C-H} (chiral center) $\nu_{as\ C-F}$ (counter anion)	ρ_{C-H} (chiral center) $\nu_{as\ C-F}$ (counter anion)	ρ_{C-H} (chiral center) ν_{as} C-F (counter anion)
10	ν_{c-o} τ_{CH} (CH_3) ν_{sS-O} (counter anion)	ν_{sS-O} (counter anion)	ν_{sS-O} (counter anion)
11	ν_{sC-F} (counter anion)	ν_{sC-F} (counter anion)	ν_{sC-F} (counter anion)
12	ρ_{C-H} COCNC(ring)	ρ_{C-H} COCNC(ring)	ρ_{C-H} COCNC(ring)
a	-	ν_s C-O	ν_s C-O
b	-	ν C-C-C	ν C-C-C
c (intense)	-	ν_{as} C-O	ν_{as} C-O
d	-	ρ_{C-H}	ρ_{C-H}

* Assignment was performed on the basis of DFT calculation. The PCM model was applied to account for the solvent effect ($CHCl_3$).